HHS Public Access

Author manuscript

*New Phytol*. Author manuscript; available in PMC 2023 January 01.

Published in final edited form as:

*New Phytol*. 2022 January ; 233(2): 878–889. doi:10.1111/nph.17806.

# Dissecting the labdane-related diterpenoid biosynthetic gene clusters in rice reveals directional cross-cluster phytotoxicity

**Riqing Li**[1,†], **Juan Zhang**[2,†], **Zhaohu Li**[3,4,*], **Reuben J. Peters**[2,*], **Bing Yang**[1,5,*]

[1]Division of Plant Sciences, Bond Life Sciences Center, University of Missouri, Columbia, MO 65211, USA

[2]Roy J. Carver Department of Biochemistry, Biophysics and Molecular Biology, Iowa State University, Ames, IA 50011

[3]State Key Laboratory of Physiology and Biochemistry, College of Agronomy and Biotechnology, China Agricultural University, Beijing 100193, China

[4]College of Plant Science and Technology, Huazhong Agricultural University, Wuhan 430070, China

[5]Donald Danforth Plant Science Center, St. Louis, MO 63132, USA

## Summary

- Rice (*Oryza sativa*) is a staple food crop and serves as a model cereal plant. It contains two biosynthetic gene clusters (BGCs) for production of labdane-related diterpenoids (LRDs), which serve important roles in combating biotic and abiotic stresses. While plant BGCs have been subject to genetic analyses, these have been largely confined to investigation of single genes.
- CRISPR/Cas9-mediated genome editing was used to precisely remove each of these BGCs, as well as simultaneously knock-out both BGCs.
- Deletion of the BGC from chromosome 2 (c2BGC), which is associated with phytocassane biosynthesis, but not that from chromosome 4 (c4BGC), which is associated with momilactone biosynthesis, led to a lesion mimic phenotype. This phenotype is dependent on two closely related genes encoding cytochrome P450 (CYP) mono-oxygenases, *CYP76M7* and *CYP76M8*, from the c2BGC. However, rather than being redundant, *CYP76M7* has been associated with production of phytocassanes, while *CYP76M8* is associated with momilactone biosynthesis. Intriguingly, the lesion mimic phenotype is not present in a line with both BGCs deleted.

*Correspondence: lizhaohu@cau.edu.cn, rjpeters@iastate.edu and yangbi@missouri.edu.
†These authors contributed equally to this article.

Author Contributions

R.L. and J.Z. designed and performed experiments. Z.L., R.J.P. and B.Y. conceived the project and obtained financial support. R.L. and J.Z. wrote the initial draft of the manuscript, R.J.P., Z.L. and B.Y. revised the manuscript. R.L. and J.Z. contributed equally to this work.

- These results reveal directional cross-cluster phytotoxicity, presumably arising from accumulation of LRD intermediates dependent on the c4BGC in the absence of *CYP76M7* and *CYP76M8*, further highlighting their interdependent evolution and the selective pressures driving BGC assembly.

**Keywords**

phytoalexin; CRISPR; diterpenoid; gene cluster; rice; disease resistance

## Introduction

As the staple food for over half of the global population, rice is a critically important crop (Muthayya et al., 2014). In addition, rice serves as a model cereal plant due in no small part to the small size of its genome, which led to early sequencing (Goff et al., 2002; Yu et al., 2002). Among the early findings from the rice genome sequence was the presence of two biosynthetic gene clusters (BGCs), associated with production of antimicrobial phytoalexins, which were among the first to be reported (Nutzmann et al., 2016). More specifically, these contained genes encoding enzymes for biosynthesis of labdane-related diterpenoids (LRDs), which have long been postulated to serve as phytoalexins and allelochemicals in rice (Peters, 2006), with recent results demonstrating roles in resistance to abiotic as well as biotic stresses (Lu et al., 2018; Zhang et al., 2021). Indeed, LRDs are now known to serve such roles in cereal crops more generally (Murphy & Zerbe, 2020), further emphasizing their importance.

The LRDs are characterized by initial bicyclization of the general diterpenoid precursor (*E,E,E*)-geranylgeranyl diphosphate (GGPP) catalyzed by class II diterpene cyclases (Peters, 2010). These cyclases most often produce the eponymous labdadienyl/copalyl diphosphate (CPP), leading to designation of the relevant enzymes as CPP synthases (CPSs). CPP can be produced in different stereochemical configurations, with the production of *ent*-CPP required in all vascular plants (tracheophytes) for gibberellin (GA) phytohormone biosynthesis (Zi et al., 2014). Rice also produces *syn*-CPP and LRD phytoalexins derived from this, but also from *ent*-CPP (Peters, 2006). Further cyclization and/or rearrangement of CPP is catalyzed by class I diterpene synthases, again with all tracheophytes necessarily containing an *ent*-kaurene synthase (KS) for GA biosynthesis, which has given rise to evolutionarily derived enzymes termed KS-like (KSL) (Zi et al., 2014).

The rice genome was found to contain two biosynthetic gene clusters (BGCs), defined as proximal unrelated genes involved in a common biosynthetic pathway, for LRDs, with one on chromosome (chr.) 2 (c2BGC), and the other on chr. 4 (c4BGC) (Schmelz et al., 2014). These BGCs contain not only sequentially acting CPSs and KSLs, but also cytochrome P450 (CYP) mono-oxygenases as well as, in the case of the c4BGC, short chain alcohol dehydrogenases (Fig. 1). Notably, the c4BGC is clearly associated with momilactone biosynthesis, while the c2BGC is largely associated with phytocassane biosynthesis, representing the two most prevalent LRDs produced by rice (Yamane, 2013), although the c2BGC also clearly contains both KSLs and CYPs involved in additional LRD metabolism (Swaminathan et al., 2009; Wu et al., 2011).

The occurrence of BGCs, proximal unrelated genes involved in a common biosynthetic pathway, is somewhat unusual in eukaryotic genomes (Nutzmann et al., 2018). These seem to be associated with the production of secondary metabolites not required for normal growth and development. However, not all such biosynthetic pathways are associated with BGCs, leaving the evolutionary pressures underlying their assembly in question. This has been suggested to arise from a combination of positive and negative selection pressures, both for production of bioactive metabolites but also against accumulation of certain intermediates (Swaminathan et al., 2009; Takos & Rook, 2012). Indeed, investigation of the rice c4BGC provided the first evidence for such negative effects from incomplete pathway inheritance, as a T-DNA insertion knock-out mutant of *OsKSL4* was found to exhibit significantly reduced seed germination rates (Xu et al., 2012). Notably, this study also utilized a T-DNA insertion knock-out mutant of *OsCPS4*, but found that the momilactones seemed to primarily act as allelochemicals rather than in defense against the fungal blast pathogen *Magnaporthe oryzae* (Xu et al., 2012), at least in the relevant cultivar (cv) Zhonghua 11, despite the fact that these were the first phytoalexins against *M. oryzae* found in rice (Cartwright et al., 1981). On the other hand, a T-DNA insertion knock-down mutant of *OsCPS4* found in a different rice cv (Nipponbare) did effect resistance to *M. oryzae* as well as allelopathic activity (Toyomasu et al., 2014).

Other genetic studies have been directed at these rice BGCs, albeit also primarily targeted at single genes or a pair of closely related paralogs to investigate the role of the encoded enzyme(s) in LRD biosynthesis, and occasionally that of the resulting LRDs in microbial disease resistance, rather than probing BGC evolution per se. For example, consistent with their localization within the c4BGC, RNA-interference (RNAi) mediated knock-down of the closely related *CYP99A2* and *CYP99A3* provided the first evidence that these play a role in momilactone biosynthesis (Shimura et al., 2007). Similarly, consistent with their localization within the c2BGC, RNAi knock-down of the closely related *CYP76M7* and *CYP76M8* was used to indicate that these play a role in phytocassane biosynthesis (Wang et al., 2012). Correlation of the c2BGC to phytocassane production was further bolstered by the finding that a T-DNA insertion knock-out mutant of the similarly c2BGC localized *CYP71Z7* was deficient in a certain transformation (hydroxylation at carbon-2) in the underlying metabolic network (Ye et al., 2018). Finally, the potential redundancy of *ent*-CPP derived LRD metabolism in rice was investigated using a T-DNA insertion knock-out mutant of *OsCPS2*, revealing that this is insufficient to completely block production of the phytocassanes or other *ent*-CPP derived LRDs, presumably due to the presence of the *OsCPS1* required for GA phytohormone biosynthesis, which enables continued production of *ent*-CPP (Lu et al., 2018). This study also further investigated the role of rice LRDs in microbial disease resistance, including use of the *OsCPS4* T-DNA insertion knock-out mutant, which uncovered a role for *syn*-CPP derived (*OsCPS4* dependent) LRDs in non-host disease resistance to *Magnaporthe poae*, as well as roles for *OsCPS2* associated (*ent*-CPP derived) LRDs in defense against bacterial leaf blight pathogen *Xanthomonas oryzae* pathovar *oryzae* (*Xoo*) as well as *M. oryzae* (Lu et al., 2018).

Development of the CRISPR/Cas9 technique offers precise genome editing that has now been applied to rice (Char et al., 2019), and even more specifically to its LRD BGCs in work targeted at the fast-growing cv Kitaake. In particular, this approach is most often applied

to target single genes and has been used in this context to provide direct comparison of knocking-out *OsCPS2* and/or *OsCPS4* in the same genetic background, with crossing of the initially generated *cps2* and *cps4* single-mutant lines to generate a *cps2x4* double-mutant line (Zhang et al., 2021). Similarly, the closely related *CYP76M7* and *CYP76M8* also have been individually knocked-out, revealing that *CYP76M7* is primarily associated with phytocassane biosynthesis, while *CYP76M8* is more important for momilactone production, although these do appear to be partially redundant (Kitaoka et al., 2021). However, the co-localization of these two genes in the c2BGC essentially blocks production of a double mutant line by genetic crossing. Fortunately, CRISPR/Cas9 can be applied to simultaneously target multiple genes/loci (Bi and Yang, 2017), enabling investigation of neighboring genes such as those found in BGCs, or even removal of large fragments such as entire BGCs (Li et al., 2019). Indeed, deletion of the rice LRD BGCs using CRISPR/Cas9 has previously been reported in protoplasts and, for deletion of the c2BGC, in T0 plants, although this was only present in mono-allelic form with the ~245 kb deletion paired with small nucleotide changes at the targeted sites in the other copy of the c2BGC (Zhou et al., 2014).

Here we report that deletion of the c2BGC, as well as the c4BGC, yields lines that are viable and genetically stable in homozygous form. This enabled chemotypic and phenotypic investigation of such complete BGC loss, revealing not only the expected effects on rice LRD metabolism and microbial disease resistance, but also discovery of a lesion mimic phenotype for homozygous c2BGC deletion plants. CRISPR/Cas9 multiplex targeting was then used to demonstrate that the lesion mimic phenotype depends on both *CYP76M7* and *CYP76M8*, as exhibited by the *cyp76m7/8* double, but not *cyp76m7* or *cyp76m8* single, mutant lines. Intriguingly, it was further possible to cross the BGC deletion lines to create a viable line missing both BGCs, which no longer exhibits the lesion mimic phenotype. This indicates that the lesions arise from directional phytotoxicity, presumably from c4BGC dependent LRD intermediates that accumulate in the absence of the c2BGC, specifically loss of *CYP76M7* and *CYP76M8*.

## Materials and Methods

### Plant Materials and Growth Conditions

The *japonica* cultivar (*Oryza sativa*) Kitaake was used here. The T0 plants with each BGC deleted were generated previously using CRISPR/Cas9 genome-editing (Zhou et al., 2014; Li et al., 2019). Rice seeds were sterilized in 2% sodium hypochlorite and grown aseptically on 1/2 MS medium containing 3% sucrose and 0.5% agar (pH 5.8) in plastic container at 30 °C. Two-week old seedlings were transferred and planted to big plastic boxes containing farm soil and grown in greenhouse (unless otherwise indicated). Growth conditions were 30 °C in daytime, 28 °C in nighttime, and with a 13-hour day length.

### Phytochemical Analyses

Three-week old rice leaves were cut into 5 cm pieces and 0.1 g induced by floating on a solution of 0.5 mM $CuCl_2$. After 72 h these induced leaves were frozen by submersion into liquid $N_2$ and ground into fine power, which were extracted by shaking in 3 mL methanol for 72 h in a cold (4 °C) room. Each sample had 2.31 μg sclareol added as an internal

standard. The methanol was filtered through a 0.2 μm nylon filter (F2513-2, Thermo) using a glass syringe, dried under a stream of $N_2$ gas, and resuspended in 1 mL methanol for analysis.

Analyses were carried out via LC-MS/MS, with 15 μL samples injected onto a Supelco (Sigma-Aldrich, St. Louis, MO, USA) Ascentis C18 column (10 cm x 2.1 mm; 3 μ) using an Agilent Technologies 1100 Series HPLC system coupled to both a UV-Vis diode array detector and an Agilent Technologies Mass Selective Trap SL detector located in the Iowa State University W.M. Keck Metabolomics Research Laboratory. A binary gradient was used, consisting of water with 0.1% acetic acid v/v (buffer A) and acetonitrile with 0.1% acetic acid v/v (buffer B). The solvent gradient elution was programmed as follows: initial, 40% buffer B; 0-13 min, a linear gradient from 40% buffer B to 85% buffer B; 13-14 min, a linear gradient from 85% buffer B to 100% buffer B; 14-14.5 min, a linear gradient from 100% buffer B to 40% buffer B. The known rice LRD phytoalexins were detected by MS/MS analysis, using an isolation selection window of ± 0.5 m/z. The isolated masses were reionized and the resulting mass spectra recorded.

The isolated parent ions and quantified secondary ions, along with corresponding retention time (RT), based on optimization with the available authentic standards, for the known rice LRD phytoalexins were as follows: momilactone A, m/z 315.2—271.2, RT 11.1 min; momilactone B, m/z 331.2—269.2, RT 9.0 min; oryzalexin A, m/z 303.2—285.2, RT 10.0 min; oryzalexin B, m/z 303.3—286.2, RT 9.7 min; oryzalexin C, m/z 301.2—283.2, RT 9.6 min; oryzalexin D, m/z 287.2—269.2 (147.2), RT 9.6 min; oryzalexin E, m/z 287.2—269.2, RT 11.3 min; oryzalexin S, m/z 287.2—269.2 (241.2), RT 9.7 min; phytocassane A, m/z 317.2—299.2, RT 7.6 min; phytocassane B, m/z 335.2—317.2, RT 7.3 min; phytocassane C, m/z 319.2—301.2, RT 6.8 min; phytocassane D, m/z 317.2—299.2, RT 9.7 min; phytocassane E, m/z 317.2—299.2, RT 8.3 min; phytocassane F, m/z 333.2—315.2, RT 7.3 min; sclareol, m/z 273.2—163.1, RT 13.6 min. The relative amount of each LRD was determined with the 6300 Series Ion Trap LC/MS version 1.8 software package (Bruker), by comparison of total ion peak areas to that of the sclareol internal standard.

## Fungal Resistance Assays

*M. oryzae* strains CA89 and O254 were used, and infection assays were performed as previously described (Sesma and Osbourn, 2004). Briefly, rice seedlings at the third leaf stage were used for infection. Four pots of 20 plants were used per line and per experiment. Each pot was sprayed with 5 mL of a suspension of $10^5$ conidia per milliliter. The sprayed plants were then incubated in the growth chamber with humid conditions (85% relative humidity, 25°C, and a 16-h-light/8-h-dark photoperiod) for six days to score disease symptoms. Leaf lesions were scanned and analyzed with Assess 2.0 software (American Phytopathological Society). Blast lesions were evaluated based on lesion number and lesion extension of disease symptoms as previously reported (Tucker *et al.*, 2010). One-way ANOVA statistical analyses were performed to compare wild-type and Δ*c2bgc* and Δ*c4bgc* plants. The Dunnett's significant difference test was used for post-ANOVA pairwise analysis of significance, set at 5% ($p < 0.05$).

## Bacterial Resistance Assays

*Xanthomonas oryzae* pv. *oryzae* (*Xoo*) stain PXO99$^{A}$ and its *hrpC*, a gene encoding a type III secretion system, mutant PXO99$^{A}$ME7 (ME7, for short) were used for leaf blight disease assays. *Xoo* was grown for 2 to 3 d on TSA (1% [w/v] Tryptone, 1% sucrose, 0.1% glutamic acid, and 1.5% agar, pH 6.8) plates at 28°C, scraped off, and resuspended in sterile deionized water. The suspension was then adjusted to an optical density of 0.5 at 600 nm before infection. Two-week-old seedlings were inoculated using a needleless syringe infiltration method (Zhu et al., 1998), with five infiltrated spots on each leaf. The leaves were then harvested two days after injecting and ground sufficiently in a sterile mortar by adding certain volume of sterile water. The subsequent solution was serially diluted and spread on TSA plates to count colonies, then convert into colony formation units per infiltration spot. Bacterial counting was performed three times in parallel for each rice line. One-way ANOVA statistical analyses were applied to compare wild-type and Δ*c2bgc* and Δ*c4bgc* plants after bacterial inoculation. The Dunnett's significant difference test was used for post-ANOVA pairwise analysis of significance, set at 5% ($p < 0.05$) (Fig. 4a,b,c, **see later**).

Eight-week-old rice plants were inoculated using the leaf-tip-clipping method (Kauffman et al., 1973). Symptoms were scored by measuring lesion lengths after 14 days for the leaf-clipping inoculations. Lesion length measurements are averages of 20 leaves. Lesion length of Δ*c2bgc* mutant plants was compared to WT plants after PXO99$^{A}$ inoculation. ***$p < 0.001$, calculated using post-ANOVA pairwise analysis of significance with the Dunnett's test (Fig. 5g, **see later**).

For *in vitro* antimicrobial activity assays, 150 germinated seeds each rice line were grown in a sterile beaker with 10 mL of 1/2 MS medium for 15 days in 30 °C growth chamber. The liquid solution containing root exudates from each line was collected separately. Liquid TSA medium containing 50% (V/V) of the root exudates was used for *Xoo* culture. The initial *Xoo* suspension was adjusted to an optical density (OD) of 0.15 at 600 nm and then grown in 30 °C shake incubator. $OD_{600}$ values was collected at the specified time points for growth curve of bacteria.

## DAB Staining

For measurement of $H_2O_2$ accumulation, leaves were collected at 45 days after germination and immediately submerged in a solution containing 1 mg/mL DAB (3,3'-Diaminobenzidine), and then incubated at room temperature in dark for 8 hours. The stained leaves were then decolored in 95% boiling ethanol for 10 min and soaked for two days in 95% ethanol until all chlorophyll had been removed.

## RNA Isolation and Gene Expression Analysis

Total RNA was extracted by using Trizol reagent (Thermo Fisher Scientific) according to the manufacturer's instructions. First strand cDNA synthesis for RT-PCR was carried out by using iScript™ cDNA Synthesis kit (Bio-Rad) and random primers. Real-time PCR reaction was conducted in CFX96 Touch Real-Time PCR Detection System (Bio-Rad) using SYBR

Green Supermix (Bio-Rad) according to the manufacturer's instructions. The primer pairs used to specifically amplify target genes and *Actin1* are listed in Table S3 **(see later)**.

### Genome Editing and Mutant Creation

CRISPR editing was used to mutate *CYP76M7* and *CYP76M8* genes. The CRISPR/Cas9 protocol was described previously (Zhou et al., 2014). Two guide RNA sequences targeting both *CYP76M7* and *CYP76M8* genes were designed, synthesized and used for the CRISPR/Cas9 construct, so as to mutate both genes simultaneously. Immature embryo-derived callus cells of rice (cv Kitaake) were transformed using the *Agrobacterium*-mediated rice transformation method. Transformed calli and regenerated plantlets were selected on media containing hygromycin B. T0 lines were used for mutation screening, and T-DNA free homozygous mutant lines were selected in corresponding T1 and T2 generation plants. The sequences of guide RNA and the corresponding primers used for mutation detection and plant genotyping are listed in Table S1.

## Results

### Hereditary stability of BGC deletions

To further investigate the genetic stability of the BGC deletions the previously reported T0 lines (Zhou et al., 2014) were selfed to generate T1 and T2 generations, with single plants homozygous for deletions of c2BGC or c4BGC and free of CRISPR constructs selected by PCR analysis. Specifically, for analysis of the c2BGC loci, one pair of primers, F1 and R1 flanking the 5' site (located at 21662 kb of chr. 2), and another pair of primers, F2 and R2 flanking the 3' site (located at 21906 kb of chr. 2), which were the locations of the sequences targeted for construction of this deletion, were designed (Fig. 1a, Table S1). PCR-amplicons are only expected with the F1 and R1 or F2 and R2 primers from wild-type genomic DNA (gDNA), while amplicons with F1 and R2 were only expected from gDNA in which this region has been deleted (Fig. 1a, Fig. S2a). Similarly, for analysis of the c4BGC, primer pairs F3 and R3, flanking the 5' site (located at 5323 kb of chr. 4) or F4 and R4, flanking the 3' site (located at 5485 kb of chr. 4) were used to detect the target sites used for this deletion, while F3 and R4 would only amplify gDNA with this ~160 kb region deleted (Fig. 1B, Fig. S2b, Table S1). Using these primers, individual plants were analyzed during this selection process. The observed 1:2:1 segregation of wild-type, heterozygous and homozygous deletions (Fig. 1c,d, Table S2) indicates the hereditary stability of the large deletion mutations of both the c2BGC and c4BGC. For each BGC, a line homozygous for the deletion that was also CRISPR/Cas9 construct free (as verified by the lack of targeted PCR amplicons) was selected for further investigation, and these are hereafter referred to as Δ*c2bgc* and Δ*c4bgc*. Further analysis of these lines by RT-PCR indicated that the genes from the relevant (deleted) BGC were no longer expressed in these plants, consistent with their loss from the genome (Fig. S3a,b). The sequences of gene-specific oligonucleotides for expression are provided in Table S3.

A mutant line homozygous for deletion of both c2GBC and c4GBC was generated by crossing Δ*c2bgc* and Δ*c4bgc* mutant lines, with selection for homozygous loss of both BGCs

via the same PCR-based approach described above (Fig. 1e). This line, with deletions of both c2GBC and c4GBC, is hereafter referred to as Δ*c2/c4bgc*.

## Effect of BGC deletions on LRD production

Given that it has been shown that rice production of LRDs can be induced by the application of copper chloride, enabling detection of most of these natural products (Lu et al., 2018), investigation of such elicited leaf extracts was utilized here. In particular, to investigate how BGC deletion affected LRD production, leaves from the Δ*c2bgc*, Δ*c4bgc* and Δ*c2/c4bgc* lines were induced and extracted, with analysis via a liquid chromatography-tandem mass spectrometry (LC-MS) method developed for this purpose (Lu et al., 2018). Consistent with the multiple genes from the c2BGC associated with phytocassane biosynthesis (Fig. 1), these LRDs were no longer detectable from Δ*c2bgc* seedlings (Fig. 2a). By contrast, consistent with the remaining presence of the relevant *OsKSL10*, as well as *OsCPS1* (Fig. S1), production of oryzalexins A – F remained essentially unaffected (Fig. 2d). On the other hand, consistent with the previously demonstrated importance of *CYP76M8* to momilactone biosynthesis (Kitaoka et al., 2021), production of these LRDs was significantly reduced (Fig. 2b). Perhaps reflecting increased availability of *syn*-CPP, production of the derived oryzalexin S was significantly increased (Fig. 2c). In Δ*c4bgc* plants, consistent with the multiple genes from this BGC associated with momilactone biosynthesis (Fig. 1), these LRDs were no longer detectable (Fig. 2b). Similarly, the *OsCPS4* dependent (*syn*-CPP derived) oryzalexin S also is essentially not produced (Fig. 2c). By contrast, production of phytocassanes was significantly increased (Fig. 2a), perhaps due to increased availability of GGPP as has been speculated for *cps* mutants (Zhang et al., 2021). On the other hand, production of oryzalexins A – F was reduced (Fig. 2d). As expected, phytocassanes, momilactones and oryzalexin S were no longer detectable in Δ*c2/c4bgc* plants, and production of oryzalexins A – F was significantly reduced (Fig. 2a,b,c,d).

## Effect on susceptibility to the fungal blast pathogen

Given the previously demonstrated differential effect of rice LRD phytoalexins on resistance to various species from the phytopathogenic fungal genus *Magnaporthe* and even strains of *M. oryzae* (Lu et al., 2018), two *M. oryzae* strains (O254 and CA89) were examined here with Δ*c2bgc* and Δ*c4bgc* mutant plants as well as the parental/wild-type (WT) cv Kitaake. The O254 strain was from India, while CA89 was from California in the US. Susceptibility was assayed by spray-inoculating rice seedlings at the 3-leaf stage and analyzing diseased (discolored) leaf area (Fig. 3). Consistent with the previous finding that the inducible *ent*-CPP derived LRDs, which are largely dependent on *OsCPS2*, are effective phytoalexins against this pathogen (Lu et al., 2018), Δ*c2bgc* and Δ*c2/c4bgc* mutant plants were significantly more susceptible to both strains, although this effect is much more pronounced with strain O254 than CA89. By contrast, Δ*c4bgc* mutant plants did not exhibit significantly increased susceptibility to either strain of *M. oryzae* (Fig. 3a,b,c,d).

## Effect on susceptibility to the bacterial leaf blight pathogen

It has previously been suggested that *OsCPS2*-dependent, *ent*-CPP derived, but not *OsCPS4*-dependent (*syn*-CPP derived), LRDs are effective against the rice bacterial leaf blight pathogen *Xoo* (Lu et al., 2018; Zhang et al., 2021). This was further examined here with

Δ*c2bgc* and Δ*c4bgc* mutant plants compared to WT, using *Xoo* strain PXO99$^{A}$ to infect two-week old seedlings via infiltration and measuring bacterial numbers two days post-infection (Fig. 4). As expected, Δ*c2bgc* and Δ*c2/c4bgc* plants were significantly more susceptible to *Xoo* (Fig. 4a), with almost a 10-fold increase in colony forming units (CFU) relative to WT (Fig. 4b), while Δ*c4bgc* plants instead exhibited a slight but significant decrease in CFU (Fig. 4a,b).

## c2BGC-dependent LRDs as phytoalexins and phytoanticipins against *Xoo*

The vast majority of rice LRDs are considered to be phytoalexins whose production is inducible (Peters, 2006), with accumulation of momilactones and phytocassanes specifically observed in *Xoo* infected leaf tissues (Klein et al., 2015). However, only the oryzalides and related (*ent*-isokaurene derived) LRDs, whose production is not strongly inducible (Watanabe et al., 1996), have been shown to exhibit antibiotic activity against *Xoo* and, hence, serve as phytoanticipins. The effectiveness of *ent*-CPP derived (*OsCPS2* dependent) LRDs has been demonstrated by the increased susceptibility of *cps2* knock-out mutant plants to infection by *Xoo* (Lu et al., 2018; Zhang et al., 2021). However, it remains unclear if this effect is due to activity of the relevant phytoanticipins (oryzalides and related LRDs) or phytoalexins (phytocassanes) against this bacterial phytopathogen. This was examined here with the *Xoo* mutant strain PXO99$^{A}$ME7 (hereafter ME7), which is incapable of type III effector secretion and considered nonpathogenic, as it does not induce the plant defense response (Sugio et al., 2007). Notably, ME7 grew at the same rate in the Δ*c2bgc*, Δ*c4bgc* and Δ*c2/c4bgc* mutant plants relative to WT (Fig. 4a,c). To verify that the c2BGC-dependent LRDs still exhibit antimicrobial activity against the *Xoo* mutant strain ME7, as well as the parental pathogenic strain PXO99$^{A}$, bioassays were performed using root exudates, which are known to contain a number of LRDs (Toyomasu et al., 2008). In particular, root exudates from WT, Δ*c2bgc*, Δ*c4bgc*, and Δ*c2/c4bgc* seedlings were collected (separately), which was added to liquid culture media then used to grow PXO99$^{A}$ and ME7 (again separately), with the growth rate observed by optical density measurements (Fig. 4d,e). Consistent with general antibiotic activity of the c2BGC-dependent LRDs against *Xoo*, both PXO99$^{A}$ and ME7 grew faster in medium with root exudates from Δ*c2bgc* and Δ*c2/c4bgc* mutant plants than with those from WT or Δ*c4bgc* mutant plants (Fig. 4d,e). The contrast between the unaffected growth of ME7 on Δ*c2bgc* mutant plants relative to the inhibitory effect of Δ*c2bgc* root exudates on ME7 growth in liquid culture indicates that rice produces c2BGC-dependent (*ent*-CPP derived) LRDs as phytoalexins against *Xoo* in their leaves. In addition, given the effectiveness of such LRDs from uninduced root exudates against *Xoo* growth, it appears that these natural products also serve as phytoanticipins in the rhizosphere.

## A lesion mimic phenotype with Δ*c2bgc* plants

Consistent with the effect recently reported for *cps2* and *cps4*, as well as *cps2x4*, knock-out mutants in cv Kitaake (Zhang et al., 2021), the Δ*c2bgc* and Δ*c4bgc* mutant plants exhibit a drought sensitive phenotype (Fig. S4). Notably, the Δ*c2bgc*, but not Δ*c4bgc* or Δ*c2/c4bgc*, mutant plants also were found to exhibit a lesion mimic phenotype about seven weeks after germination, in the booting stage (Fig. 5a). This lesion mimic phenotype was temperature sensitive, as under low-temperature growth conditions (23 °C) lesions were only rarely observed even in the heading stage of Δ*c2bgc* mutant plants (Fig. 5b).

To investigate the basis for lesion formation, leaves of the Δ*c2bgc* mutant plants were stained with 3,3 C-diaminobenzidine (DAB), with the observed formation of reddish-brown formazan precipitates indicative of $H_2O_2$ accumulation (Fig. 5c). Such reactive oxygen species can trigger either necrosis or programed cell death (VanBreusegem & Dat, 2006), with the more specific hypersensitive response further coupled to defense responses (Balint-Kurti, 2019), which is often associated with lesion mimic mutants (Bruggeman et al., 2015). Thus, it was hypothesized that defense against pathogens in Δ*c2bgc* mutant plants might be enhanced. This was first investigated by analysis of the expression level of rice defense-related genes, including *PBZ* (Kim et al., 2004), *PR1* (Mitsuhara et al., 2008) and inducible peroxidase *POX22-3* (Chittoor et al., 1997), in Δ*c2bgc* leaves before and after lesion appearance. All the defense-related genes were significantly up-regulated in Δ*c2bgc* mutant leaves with appearance of the lesions, with no change in expression levels in Δ*c4bgc* and Δ*c2/c4bgc* mutant or WT plants during the same growth stage (Fig. 5d,e,f). Indeed, following lesion formation the Δ*c2bgc* mutant plants exhibited enhanced resistance against *Xoo* PXO99$^A$ relative to WT at the same growth stage (Fig. 5g,h). These results indicate that the lesion mimic phenotype exhibited by loss of the c2BGC arises from a hypersensitive response that appears latter in rice plant development.

### *CYP76M7* and *CYP76M8* are responsible for lesion mimic phenotype

To determine the gene(s) from the c2BGC responsible for the lesion mimic phenotype the relevant previously reported cv Kitaake mutant lines were examined – i.e., *cps2* (Zhang et al., 2021), as well as *cyp76m7* and *cyp76m8* (Kitaoka et al., 2021). However, none of these single gene knock-outs exhibited this phenotype. Fortuitously, it was recently noted that RNAi knock-down of the closely related paralogs *CYP76M7* and *CYP76M8* from the c2BGC led to a lesion mimic phenotype (Ye et al., 2018). Thus, a multiplex CRISPR/Cas9 approach was used to knock-out both genes simultaneously (Fig. S5), with the resulting *cyp76m7/8* double-mutant plants found to exhibit the lesion mimic phenotype (Fig. 6a), as well as drought sensitivity (Fig. S6). Like Δ*c2bgc* mutant plants, this lesion mimic phenotype was temperature sensitive, as under low-temperature growth conditions (23 °C) lesions were similarly only rarely observed even in the heading stage (Fig. 6b). DAB staining of *cyp76m7/8* double-mutant leaves was observed to form reddish-brown formazan, indicating accumulation of $H_2O_2$ (Fig. 6c). The expression level of rice defense-related genes, including *PBZ*, *PR1* and *POX22-3*, also was found to be remarkedly increased (Fig. 6d,e,f). Accordingly, the *cyp76m7/8* double-mutant then seems to be sufficient to induce the same hypersensitive response seen with Δ*c2bgc* plants.

Investigation of secreted LRDs demonstrated that the *cyp76m7/8* double-mutant has significant reductions of both phytocassanes or momilactones, with no consistent effect on either oryzalexin S or oryzalexins A – F (Fig. 6g,h,i,j). Although both phytocassanes and momilactones were significantly reduced in *cyp76m7/8* double-mutant plants, the lesion mimic phenotype does not appear to be due to reduction of LRD accumulation. In particular, despite similar reductions in these prevalent LRDs, the *cps2x4* (Zhang et al., 2021) and Δ*c2/c4bgc* (Fig. 5a, Fig. 7) double mutants do not display a lesion mimic phenotype. This contrast indicates that the LRDs are not simply acting as antioxidants – i.e., to block accumulation of reactive oxygen species.

## Discussion

While deletion of the two BGCs for LRD production in rice has been previously reported in heterozygous form (Zhou et al., 2014), the results reported here demonstrate that this removal of substantial portions of the genome, and loss of associated biosynthetic capacity, is genetically stable. The effects of these deletion mutants on LRD production are consistent with the previously reported role of the *CYP76M* subfamily members (especially *CYP76M8*) from the c2BGC in momilactone biosynthesis, which is otherwise associated with the c4BGC (Kitaoka et al., 2021). The ability of Δ*c2bgc* mutant plants to produce some momilactones presumably is due to the previously reported ability of CYP76M14, located elsewhere in the genome, to catalyze the equivalent reaction (Kitaoka et al., 2021). This contrasts with the essentially complete loss of momilactone production exhibited by *cyp76m7/8* double-mutant lines, which may be explicable by the inefficiency of the other CYP76M subfamily members in catalyzing the relevant reaction. In particular, when only *CYP76M7* and *CYP76M8* are knocked-out, rather than deletion of the whole c2BGC, other substrates with which the remaining CYP76M subfamily members exhibit greater catalytic efficiency may then be present, preventing these from acting in momilactone biosynthesis. Alternatively, this effect may be due to altered expression of these subfamily members in Δ*c2bgc* mutant plants relative to the *cyp76m7/8* double-mutant lines.

The effects of the two BGC deletion mutants on microbial disease resistance also was consistent with previously reported results (Lu et al., 2018; Zhang et al., 2021). However, the results from the *Xoo* bioassays reported here demonstrate that the c2BGC-dependent (*ent*-CPP derived) LRDs exhibit direct antibiotic activity against this bacterial pathogen. Moreover, it also is now evident that these natural products serve as phytoalexins in the leaves as well as phytoanticipins in the rhizosphere. In addition, the c2BGC-dependent (*ent*-CPP derived) LRDs exhibit differential effects on fungal blast resistance with the two strains of *M. oryzae* used here. Given that the LRD phytoalexins accumulate significantly faster in resistant relative to susceptible rice cultivars (Hasegawa et al., 2010), it appears that the relevance of the LRD phytoalexins to the defense response depends on timely detection of the microbial pathogen by the rice host. Thus, the differential results are presumably due to partial genetic (in)compatibility between cv Kitaake rice and the *M. oryzae* strains used here, just as seen in other known plant-pathogen interactions (Delplace et al., 2021).

The effect of the BGC deletion mutants on drought resistance again is consistent with previously reported results (Zhang et al., 2021). In particular, the complete loss of either phytocassanes or momilactones, the most prevalent LRDs in rice, in Δ*c2bgc* and Δ*c4bgc* mutant plants (respectively), resembles the effect of the *cps2* and *cps4* knock-out mutants in which this phenotype was first observed. This supports the hypothesis that LRDs act as a regulatory switch, with accumulation above a certain threshold promoting stomatal closure (Zhang et al., 2021). The *cyp76m7/8* double knock-out mutant lines, with significant reductions in both phytocassanes and momilactones, also exhibit this phenotype, again consistent with this hypothesis.

Perhaps most interesting is the observation of a lesion mimic phenotype with Δ*c2bgc* mutant plants. The results reported here indicate that this results from a hypersensitive response,

which includes induction of the rice microbial defense response. Fortuitously, it was possible to dissect the c2BGC and identify the relevant genes for this phenotype as the closely related *CYP76M7* and *CYP76M8*. Intriguingly, despite exhibiting similar catalytic activity in recombinant settings, these are not redundant, with *CYP76M7* serving a more important role in phytocassane biosynthesis while *CYP76M8* is more important for momilactone production (Kitaoka et al., 2021). Nevertheless, only the *cyp76m7/8* double-mutant plants exhibit the lesion mimic phenotype.

It has been postulated that phytoalexins exhibit antioxidant activity, at least *in vitro* (Ahuja et al., 2012), and the loss of such antioxidants would be consistent with the observed accumulation of $H_2O_2$ during appearance of the lesion mimic phenotype. However, the lack of this phenotype in other mutant lines that exhibit analogous loss of LRD biosynthesis as Δ*c2bgc*, most markedly Δ*c2/c4bgc*, demonstrates that this is not simply due to antioxidant loss. Instead, the results suggest that phytotoxicity occurs in the absence of the c2BGC, particularly *CYP76M7* and *CYP76M8*, but requires the presence of the c4BGC, leading to a hypersensitive response. Intriguingly, it has recently been shown that knocking-down the expression of CYPs involved in diterpenoid biosynthesis can lead to accumulation of phytotoxic intermediates in *Nicotiana attenuata* (Li et al., 2021), and it seems likely that similar phytotoxic accumulation of LRD intermediates dependent on the c4BGC may occur in rice in the absence of *CYP76M7* and *CYP76M8* from the c2BGC. This is most likely due to intermediates from the c4BGC-associated momilactone biosynthesis, which has recently been elucidated (De La Pena & Sattely, 2021; Kitaoka et al., 2021), particularly the *syn*-pimaradien-19-al substrate of CYP76M8. However, given the more general role of *OsCPS4* for all *syn*-CPP derived LRDs in rice (not all of which are known; see Fig. S1), this requires further investigation.

Regardless of the underlying mechanism, the observed directional phytotoxicity between these two BGCs provides further insight into their evolution. While the role for such negative selection pressure in BGC assembly might suggest that *CYP76M7* and *CYP76M8* should have been ‘recruited’ from the c2BGC to c4BGC, this ignores their largely distinct biosynthetic roles and evolutionary history. In particular, extensive phylogenomic comparison indicates that phytocassane biosynthesis and assembly of the associated c2BGC arose first, with momilactone biosynthesis and assembly of the associated c4BGC occurring later (Miyamoto et al., 2016). Thus, the *CYP76M* subfamily member originally recruited to the c2BGC must have been involved in phytocassane production, with subsequent gene duplication giving rise to a copy that became specialized for momilactone biosynthesis (*CYP76M8*). The interdependent evolution of these two BGCs has been previously noted (Kitaoka et al., 2021). Nevertheless, the negative selection pressure (i.e., phytotoxicity) demonstrated here provides further insight on the constraints this has imposed. In particular, as this evolutionary process seems to have been sufficient to alleviate the usual recruitment that might have otherwise been expected to move *CYP76M8* to the c4BGC. In any case, it is expected that further dissection of these intriguing genetic loci will provide additional insights into the underlying mechanisms, as well as evolutionary pressures for such BGC assembly.

## Supplementary Material

Refer to Web version on PubMed Central for supplementary material.

## Acknowledgements

This work was partially supported by the US Department of Agriculture - National Institute of Food and Agriculture (grant no. 2020-67013-32557 to R.J.P and B.Y.) and the National Institutes of Health (grant no. GM131885 to R.J.B.). The authors are grateful to the National Small Grain Collection for providing rice seed, to Bo Liu and Huanbin Zhou for initially generating the gene cluster deletion lines, and to Guo-Liang Wang for kindly providing the two strains of *Magnaporthe oryzae*.

## Data Availability

Data available in article supplementary material.

## References

Ahuja I, Kissen R, and Bones AM 2012. Phytoalexins in defense against pathogens. Trends Plant Sci. 17: 73–90. [PubMed: 22209038]

Balint-Kurti P 2019. The plant hypersensitive response: concepts, control and consequences. Mol. Plant Pathol 20: 1163–1178 [PubMed: 31305008]

Bednarek P, and Osbourn A 2009. Plant-microbe interactions: chemical diversity in plant defense. Science 324: 746–748. [PubMed: 19423814]

Bruggeman Q, Raynaud C, Benhamed M, Delarue M. 2015. To die or not to die? Lessons from lesion mimic mutants. Front. Plant Sci 6: 24 [PubMed: 25688254]

Bi H, and Yang B 2017. Gene editing with TALEN and CRISPR/Cas in rice. Prog. Mol. Biol. Transl. Sci 149: 81–98. [PubMed: 28712502]

Cartwright DW, Langcake P, Pryce RJ, Leworthy DP, and Ride JP 1981. Isolation and characterization of two phytoalexins from rice as momilactones A and B. Phytochemistry 20: 535–537.

Char SN, Li R, and Yang B 2019. CRISPR/Cas9 for mutagenesis in rice. Methods Mol. Biol 1864: 279–293. [PubMed: 30415343]

Chittoor JM, Leach JE, and White FF 1997. Differential induction of a peroxidase gene family during infection of rice by *Xanthomonas oryzae* pv. *oryzae*. Mol. Plant Microbe Interact 10: 861–871. [PubMed: 9304860]

De La Pena R, Sattely ES. 2021. Rerouting plant terpene biosynthesis enables momilactone pathway elucidation. Nat. Chem. Biol 17: 205–212. [PubMed: 33106662]

Delplace F, Huard-Chauveau C, Berthome R, Roby D. 2021. Network organization of the plant immune system: from pathogen perception to robust defense induction. Plant J. doi:10.1111/tpj.15462.

Goff SA, Ricke D, Lan TH, Presting G, Wang R, Dunn M, Glazebrook J, Sessions A, Oeller P, Varma H, et al. 2002. A draft sequence of the rice genome (*Oryza sativa* L. ssp. *japonica*). Science 296: 92–100. [PubMed: 11935018]

Hasegawa M, Mitsuhara I, Seo S, Imai T, Koga J, Okada K, Yamane H, and Ohashi Y 2010. Phytoalexin accumulation in the interaction between rice and the blast fungus. Mol. Plant Microbe Interact 23: 1000–1011. [PubMed: 20615111]

Kauffman HE, Reddy APK, Hsieh SPY, and Merca SD 1973. An improved technique for evaluating resistance of rice varieties to *Xanthomonas oryzae*. Plant Dis. Rep 56:537–541.

Kim ST, Kim SG, Hwang DH, Kang SY, Kim HJ, Lee BH, Lee JJ, Kang KY. 2004. Proteomic analysis of pathogen-responsive proteins from rice leaves induced by rice blast fungus, *Magnaporthe grisea*. Proteomics 4(11): 3569–3578. [PubMed: 15478215]

Kitaoka N, Zhang J, Oyagbenro RK, Brown B, Wu Y, Yang B, Li Z, and Peters RJ 2021. Interdependent evolution of biosynthetic gene clusters for momilactone production in rice. Plant Cell 33: 290–305. [PubMed: 33793769]

Klein AT, Yagnik GB, Hohenstein JD, Ji Z, Zi J, Reichert MD, MacIntosh GC, Yang B, Peters RJ, Vela J, et al. 2015. Investigation of the chemical interface in the soybean-aphid and rice-bacteria interactions using MALDI-Mass spectrometry imaging. Anal. Chem 87: 5294–5301. [PubMed: 25914940]

Li J, Halitschke R, Li D, Paetz C, Su H, Heiling S, Xu S, and Baldwin IT 2021. Controlled hydroxylations of diterpenoids allow for plant chemical defense without autotoxicity. Science 371: 255–260. [PubMed: 33446550]

Li R, Char SN, Yang B 2019. Creating large chromosomal deletions in rice using CRISPR/Cas9. Methods Mol. Biol 1917: 47–61. [PubMed: 30610627]

Lu X, Zhang J, Brown B, Li R, Rodriguez-Romero J, Berasategui A, Liu B, Xu M, Luo D, Pan Z, et al. 2018. Inferring roles in defense from metabolic allocation of rice diterpenoids. Plant Cell 30: 1119–1131. [PubMed: 29691314]

Murphy K, Zerbe P 2020. Specialized diterpenoid metabolism in monocot crops: Biosynthesis and chemical diversity. Phytochemistry 172: 112289. [PubMed: 32036187]

Muthayya S, Sugimoto JD, Montgomery S, and Maberly GF 2014. An overview of global rice production, supply, trade, and consumption. Ann. N.Y. Acad. Sci 1324: 7–14. [PubMed: 25224455]

Mitsuhara I, Iwai T, Seo S, Yanagawa Y, Kawahigasi H, Hirose S, Ohkawa Y, Ohashi Y. 2008. Characteristic expression of twelve rice *PR1* family genes in response to pathogen infection, wounding, and defense-related signal compounds (121/180). Mol. Genet. Genomics 279(4): 415–427. [PubMed: 18247056]

Miyamoto K, Fujita M, Shenton MR, Akashi S, Sugawara C, Sakai A, Horie K, Hasegawa M, Kawaide H, Mitsuhashi W, et al. 2016. Evolutionary trajectory of phytoalexin biosynthetic gene clusters in rice. Plant J 87(3): 293–304. [PubMed: 27133567]

Nutzmann HW, Huang A, and Osbourn A 2016. Plant metabolic clusters - from genetics to genomics. New Phytol. 211: 771–789. [PubMed: 27112429]

Nutzmann HW, Scazzocchio C, and Osbourn A 2018. Metabolic gene clusters in eukaryotes. Annu. Rev. Genet 52: 159–183. [PubMed: 30183405]

Peters RJ 2006. Uncovering the complex metabolic network underlying diterpenoid phytoalexin biosynthesis in rice and other cereal crop plants. Phytochemistry 67: 2307–2317. [PubMed: 16956633]

Peters RJ 2010. Two rings in them all: the labdane-related diterpenoids. Nat. Prod. Rep 27: 1521–1530. [PubMed: 20890488]

Schmelz EA, Huffaker A, Sims JW, Christensen SA, Lu X, Okada K, and Peters RJ 2014. Biosynthesis, elicitation and roles of monocot terpenoid phytoalexins. Plant J. 79: 659–678. [PubMed: 24450747]

Shimura K, Okada A, Okada K, Jikumaru Y, Ko K-W, Toyomasu T, Sassa T, Hasegawa M, Kodama O, Shibuya N, et al. 2007. Identification of a biosynthetic gene cluster in rice for momilactones. J. Biol. Chem 282: 34013–34018. [PubMed: 17872948]

Sugio A, Yang B, Zhu T, and White FF 2007. Two type III effector genes of *Xanthomonas oryzae* pv. *oryzae* control the induction of the host genes *OsTFIIAgamma1* and *OsTFX1* during bacterial blight of rice. Proc. Natl. Acad. Sci. USA 104: 10720–10725. [PubMed: 17563377]

Swaminathan S, Morrone D, Wang Q, Fulton DB, and Peters RJ 2009. CYP76M7 is an *ent*-cassadiene C11α-hydroxylase defining a second multifunctional diterpenoid biosynthetic gene cluster in rice. Plant Cell 21: 3315–3325. [PubMed: 19825834]

Takos AM, and Rook F 2012. Why biosynthetic genes for chemical defense compounds cluster. Trends Plant Sci. 17: 383–388. [PubMed: 22609284]

Toyomasu T, Kagahara T, Okada K, Koga J, Hasegawa M, Mitsuhashi W, Sassa T, and Yamane H 2008. Diterpene phytoalexins are biosynthesized in and exuded from the roots of rice seedlings. Biosci. Biotechnol. Biochem 72: 562–567. [PubMed: 18256463]

Toyomasu T, Usui M, Sugawara C, Otomo K, Hirose Y, Miyao A, Hirochika H, Okada K, Shimizu T, Koga J, et al. 2014. Reverse-genetic approach to verify physiological roles of rice phytoalexins: characterization of a knockdown mutant of OsCPS4 phytoalexin biosynthetic gene in rice. Physiol. Plant 150: 55–62. [PubMed: 23621683]

Van Breusegem F, Dat JF. 2006. Reactive oxygen species in plant cell death. Plant Physiol. 141: 384–390. [PubMed: 16760492]

Wang Q, Hillwig ML, Okada K, Yamazaki K, Wu Y, Swaminathan S, Yamane H, and Peters RJ 2012. Characterization of CYP76M5-8 indicates metabolic plasticity within a plant biosynthetic gene cluster. J. Biol. Chem 287: 6159–6168. [PubMed: 22215681]

Watanabe M, Kono Y, Esumi Y, Teraoka T, Hosokawa D, Suzuki Y, Sakurai A, and Watanabe M 1996. Studies on a quantitative analysis of oryzalides and oryzalic acids in rice plants by GC-SIM. Biosci. Biotechnol. Biochem 60: 1460–1463.

Wu Y, Hillwig ML, Wang Q, and Peters RJ 2011. Parsing a multifunctional biosynthetic gene cluster from rice: Biochemical characterization of CYP71Z6 & 7. FEBS Lett. 585: 3446–3451. [PubMed: 21985968]

Xu M, Galhano R, Wiemann P, Bueno E, Tiernan M, Wu W, Chung IM, Gershenzon J, Tudzynski B, Sesma A, et al. 2012. Genetic evidence for natural product-mediated plant-plant allelopathy in rice (*Oryza sativa*). New Phytol. 193: 570–575. [PubMed: 22150231]

Yamane H 2013. Biosynthesis of phytoalexins and regulatory mechanisms of it in rice. Biosci. Biotechnol. Biochem 77: 1141–1148. [PubMed: 23748776]

Ye Z, Yamazaki K, Minoda H, Miyamoto K, Miyazaki S, Kawaide H, Yajima A, Nojiri H, Yamane H, and Okada K 2018. In planta functions of cytochrome P450 monooxygenase genes in the phytocassane biosynthetic gene cluster on rice chromosome 2. Biosci. Biotechnol. Biochem 82: 1021–1030. [PubMed: 29157132]

Yu J, Hu S, Wang J, Wong GK, Li S, Liu B, Deng Y, Dai L, Zhou Y, Zhang X, et al. 2002. A draft sequence of the rice genome (*Oryza sativa* L. ssp. *indica*). Science 296: 79–92. [PubMed: 11935017]

Zhang J, Li R, Xu M, Hoffmann RI, Zhang Y, Liu B, Zhang M, Yang B, Li Z, and Peters RJ 2021. A (conditional) role for labdane-related diterpenoid natural products in rice stomatal closure. New Phytol. 230: 698–709. [PubMed: 33458815]

Zhou H, Liu B, Weeks DP, Spalding MH, and Yang B 2014. Large chromosomal deletions and heritable small genetic changes induced by CRISPR/Cas9 in rice. Nucleic Acids Res. 42: 10903–10914. [PubMed: 25200087]

Zhu W, Yang B, Chittoor JM, Johnson LB, and White FF 1998. AvrXa10 contains an acidic transcriptional activation domain in the functionally conserved C terminus. Mol. Plant Microbe Interact 11: 824–832. [PubMed: 9675896]

Zi J, Mafu S, and Peters RJ 2014. To gibberellins and beyond! Surveying the evolution of (di)terpenoid metabolism. Annu. Rev. Plant Biol 65: 259–286. [PubMed: 24471837]

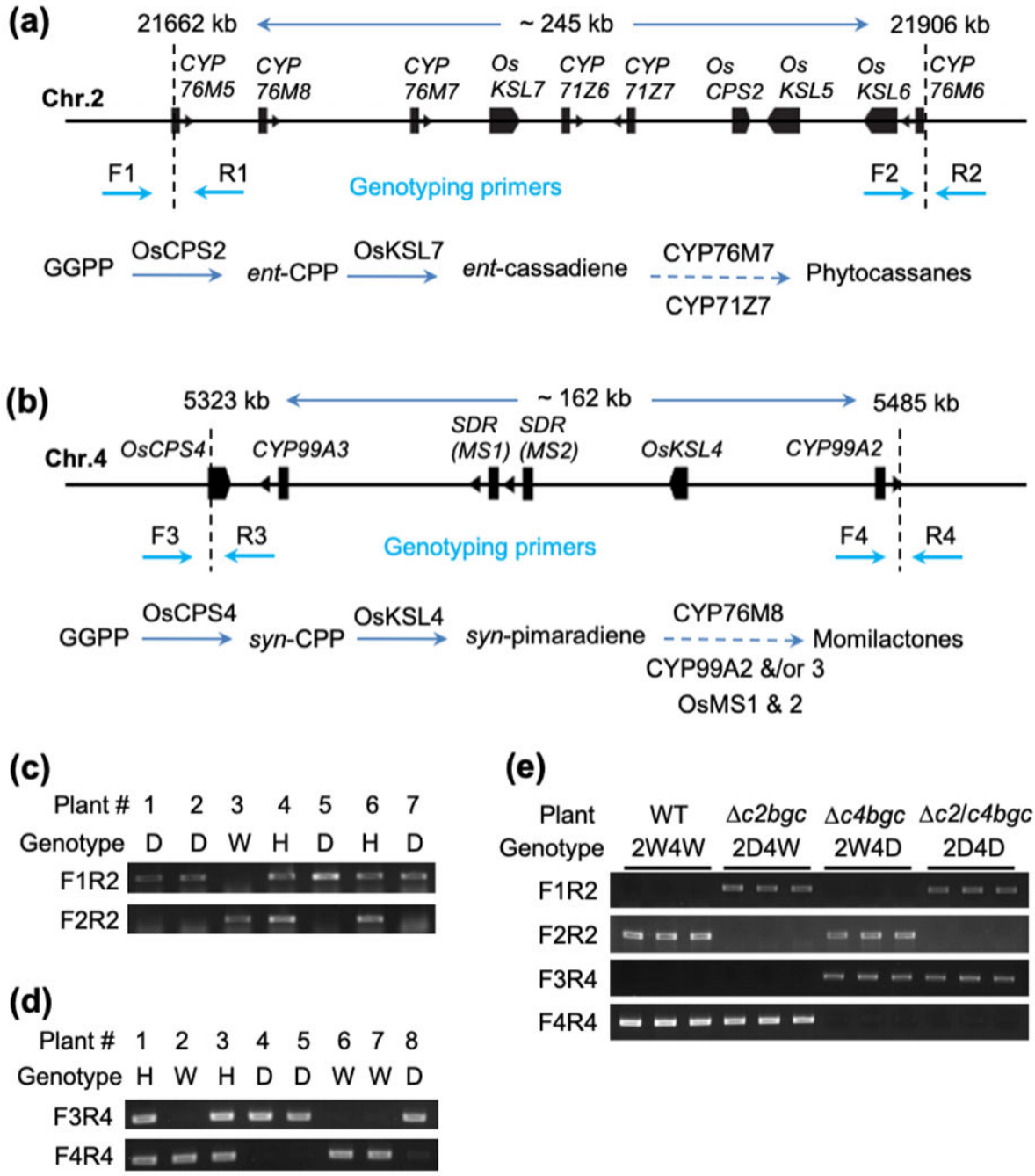


**Figure 1. Large deletions of the rice diterpenoid biosynthetic gene clusters (BGCs)**

(**a,b**) Gene structure of diterpenoid biosynthetic gene clusters on chromosome 2 (a) and 4 (b), and associated biosynthesis pathways. The filled boxes representing genes. Dashed vertical lines represent locations of genomic break sites. Dashed arrows indicate multiple enzymatic reactions leading to production of diterpenoid families (known steps shown in Fig. S1).

(**c,d,e**) Genotyping of progeny rice plants derived from the fragmental deletion mutants and their crossing using deletion-specific primers. Genotype D = mutant homozygous for

deletion, H = Heterozygous, and W = Wild-type. The number 2 and 4 in font of genotype represent Chr.2 and Chr.4, respectively

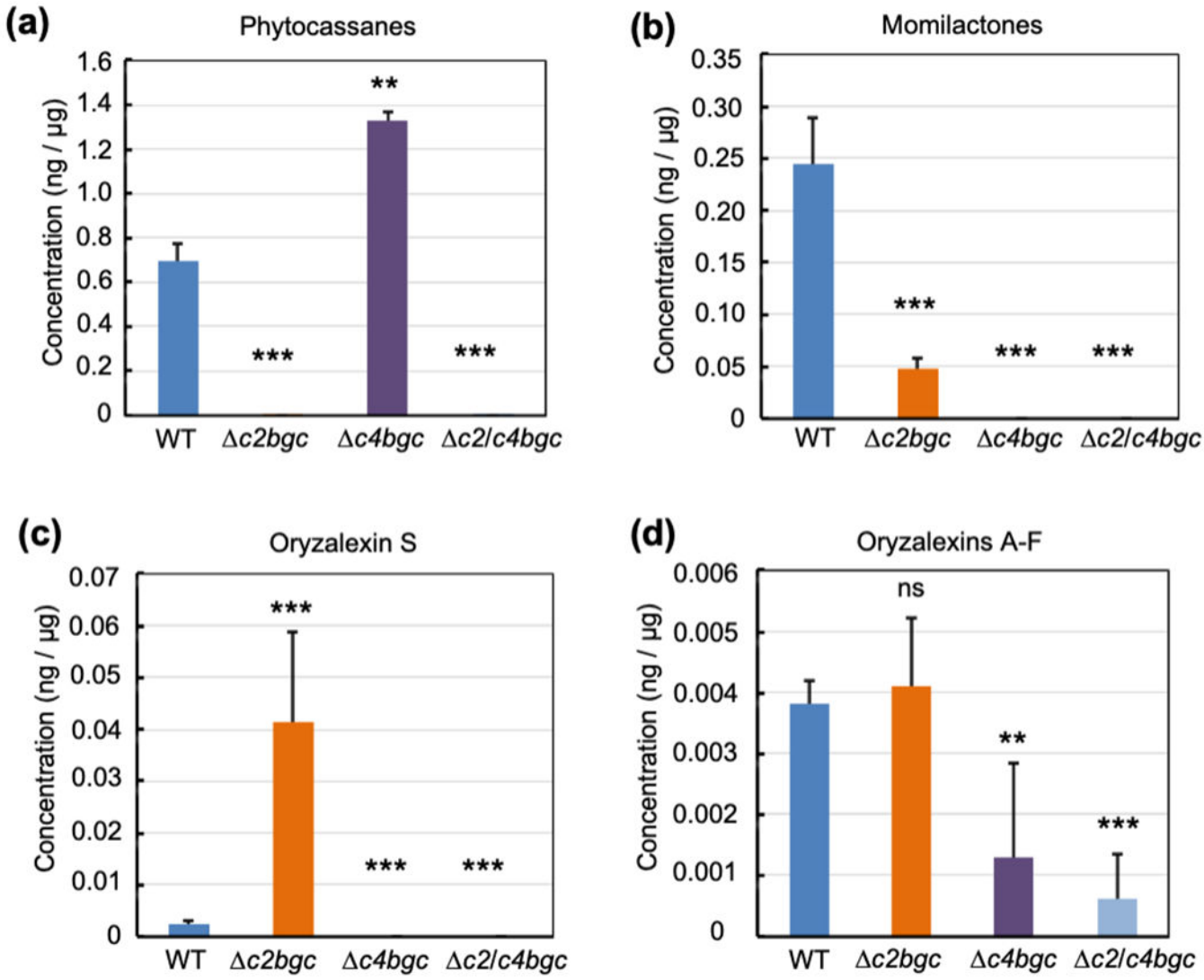


**Figure 2. Phytochemical profiling of Δ*c2bgc* and Δ*c4bgc* rice plants**

(**a,b,c,d**) Effect of deleting the c2BGC or c4BGC on labdane-related diterpenoid metabolism in rice relative to wild-type (WT) plants (average from three plants with error bars indicating standard deviation), specifically from analysis of leaves from three-week old seedlings that were induced with $CuCl_2$. *$p < 0.05$, **$p < 0.01$, ***$p < 0.001$ and ns = no significant difference, calculated using post-ANOVA pairwise analysis of significance with the Dunnette significant difference test, for Δ*c2bgc*, Δ*c4bgc* and Δ*c2/c4bgc* plants relative to the relevant wild-type line. Error bars represent +/− SD.

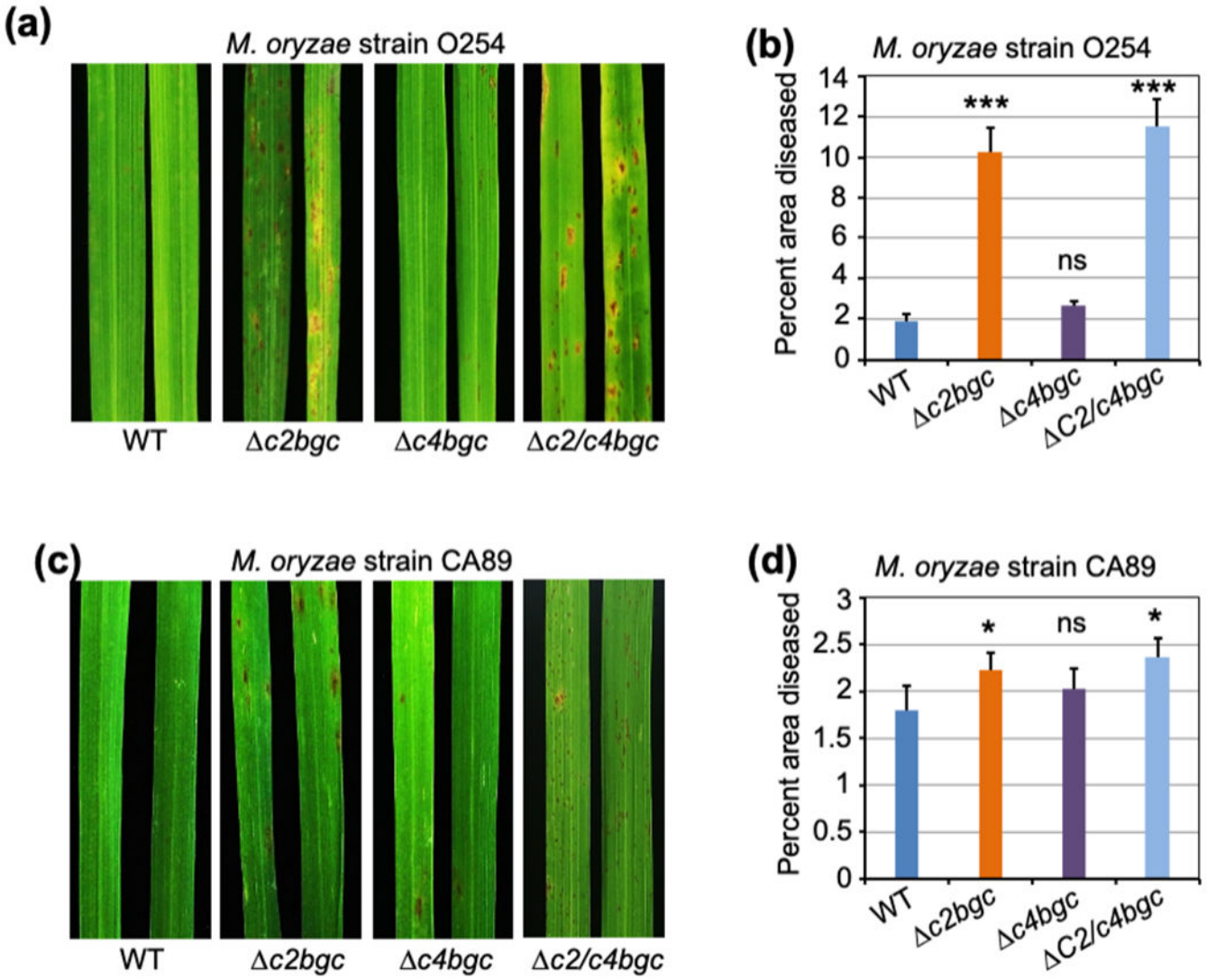


**Figure 3. Susceptibility of Δ*c2bgc*, Δ*c4bgc* and Δ*c2/c4bgc* plants against *M. oryzae***

(**a,c**) Representative leaves after infection with *M. oryzae* strain O254 (a) and CA89 (c) of rice plants at the three-leaf stage from the wild-type (WT), Δ*c2bgc*, Δ*c4bgc* and Δ*c2/c4bgc* lines as indicated.

(**b,d**) Percentage of diseased (discolored) area vs. total leaf area for Δ*c2bgc, Δc4bgc*, Δ*c2/c4bgc* and wild-type plants after infection of *M. oryzae* strain O254 (b) and CA89 (d). *$p < 0.05$, **$p < 0.01$, ***$p < 0.001$ and ns = no significant difference, calculated using post-ANOVA pairwise analysis of significance with the Dunnette significant difference test, for Δ*c2bgc* and Δ*c4bgc* plants relative to the relevant wild-type line. Error bars represent +/− SD.

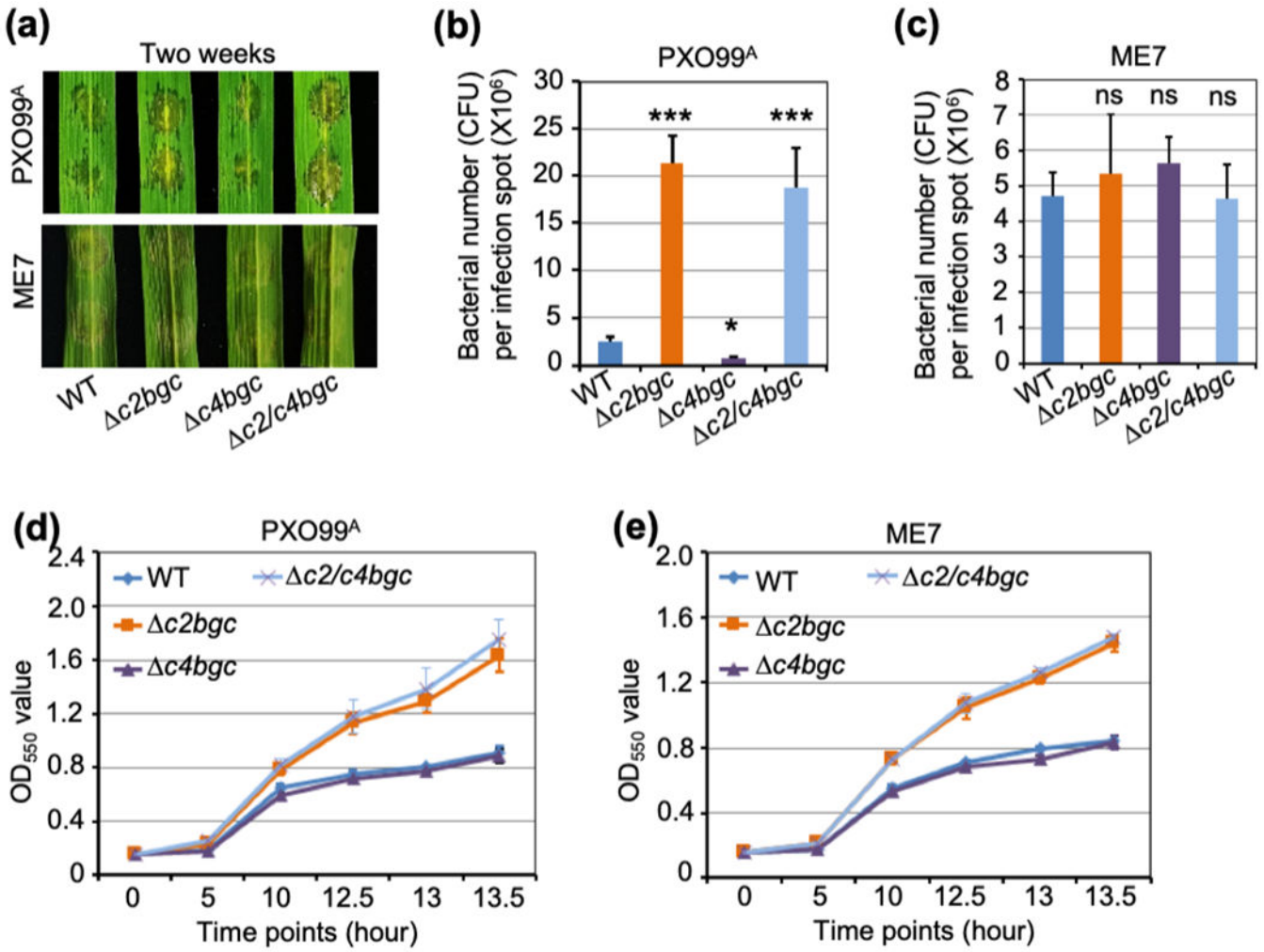


**Figure 4.** ***In vivo*** **and** ***in vitro*** **plant defense of Δ*c2bgc*, Δ*c4bgc* and Δ*c2/c4bgc* rice plants against *Xoo***

(**a**) Representative leaves from two-week old plants of the wild-type (WT), Δ*c2bgc*, Δ*c4bgc* and Δ*c2/c4bgc* lines after inoculation with PXO99$^{A}$ (upper) or the PXO99$^{A}$ME7 mutant strain (bottom) via needless syringe infiltration. ME7 is incapable of type III effector secretion, non-pathogenic and does not induce the microbial defense response in rice.

(**b,c**) Susceptibility of WT, Δ*c2bgc*, Δ*c4bgc* and Δ*c2/c4bgc* lines to infection with *Xoo* strain PXO99$^{A}$ (b) or PXO99$^{A}$ME7 (c) measured by bacterial colony counting two days post-inoculation *$p < 0.05$, **$p < 0.01$, ***$p < 0.001$ and ns = no significant difference, calculated using post-ANOVA pairwise analysis of significance with the Dunnette significant difference test, for Δ*c2bgc, Δc4bgc* and Δ*c2/c4bgc* plants relative to WT. Error bars represent +/− SD.

(**d,e**) Growth curves of PXO99$^{A}$ (d) and its mutant ME7 (e) in medium containing root exudates from WT (control), Δ*c2bgc*, Δ*c4bgc* and Δ*c2/c4bgc* mutant plants, as indicated. Error bars represent +/− SD.

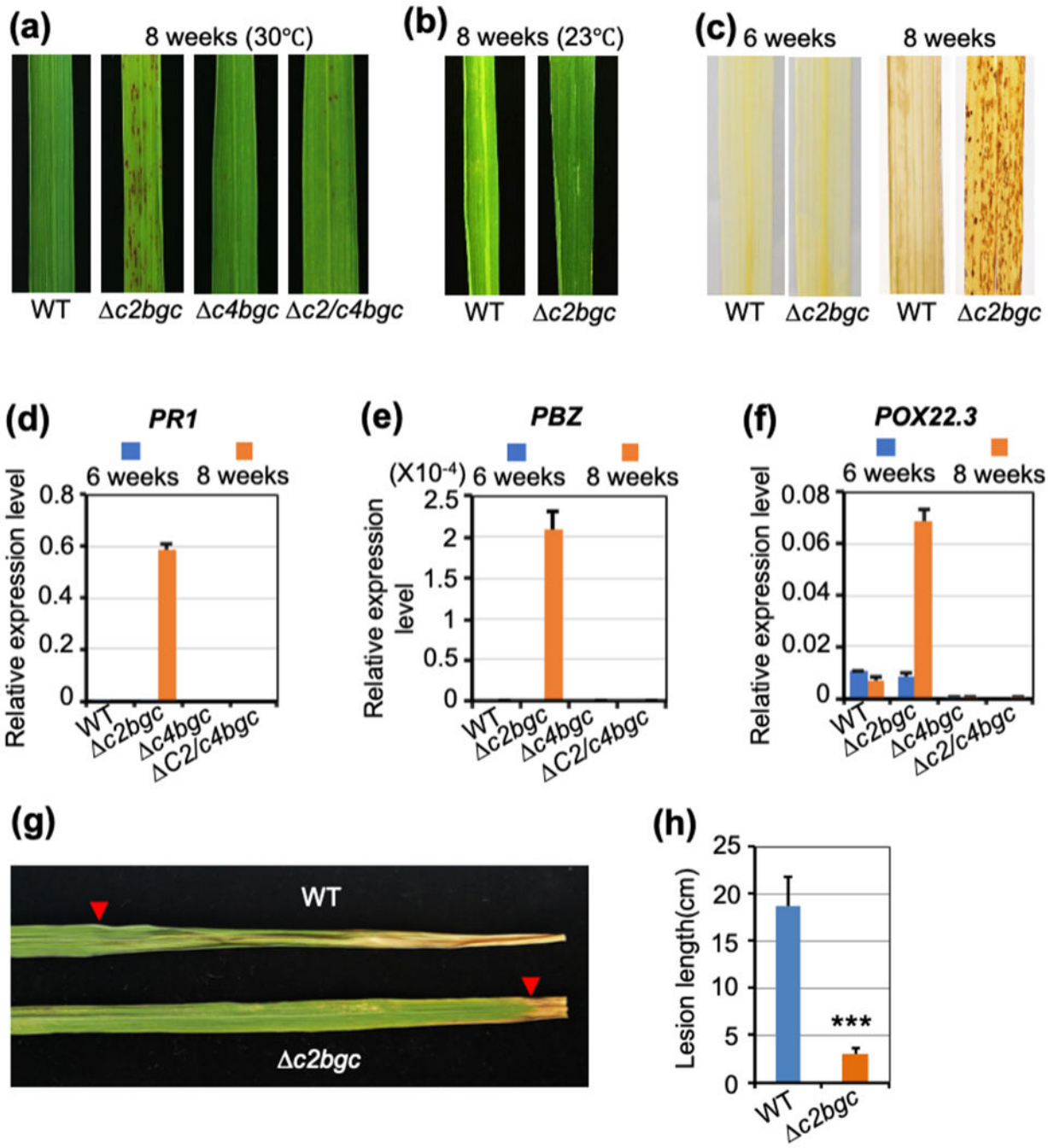


**Figure 5. Deletion of *c2BGC* leads to lesion mimic (hypersensitive response) phenotype in rice.**

(**a**) Representative leaves from wild-type (WT), Δ*c2bgc*, Δ*c4bgc* and Δ*c2/c4bgc* plants grown in greenhouse (30 °C) two months after germination.

(**b**) Representative leaves from WT and Δ*c2bgc* plants at the heading stage grown growth chamber at in 23°C.

(**c**) DAB staining of the Δ*c2bgc* mutant and WT leaves before and after appearance of lesions (i.e., the indicated time after germination).

(**d,e,f**) Relative expression level of defense-related genes, *PBZ*, *PR1* and *POX22-3* in leaves from Δ*c2bgc*, Δ*c4bgc* and Δ*c2/c4bgc* plants compared to WT. The leaf tissues were sampled before (6 wks) and after (8 wks) formation of lesions, respectively. Error bars represent +/− SD.

(**g**) Representative leaves from WT and Δ*c2bgc* eight week old plants infected with *Xoo* ($PXO99^{A}$) via the leaf-tip clipping method to distinguish lesion length from lesion mimic spots. Arrows point to the edge of the infection progression.

(**h**) Lesion length analysis for Δ*c2bgc* and WT plants after $PXO99^{A}$ inoculation. ***$p <$ 0.001, calculated using post-ANOVA pairwise analysis of significance with the Dunnette significant difference test for Δ*c2bgc* plants relative to WT. Error bars represent +/− SD.

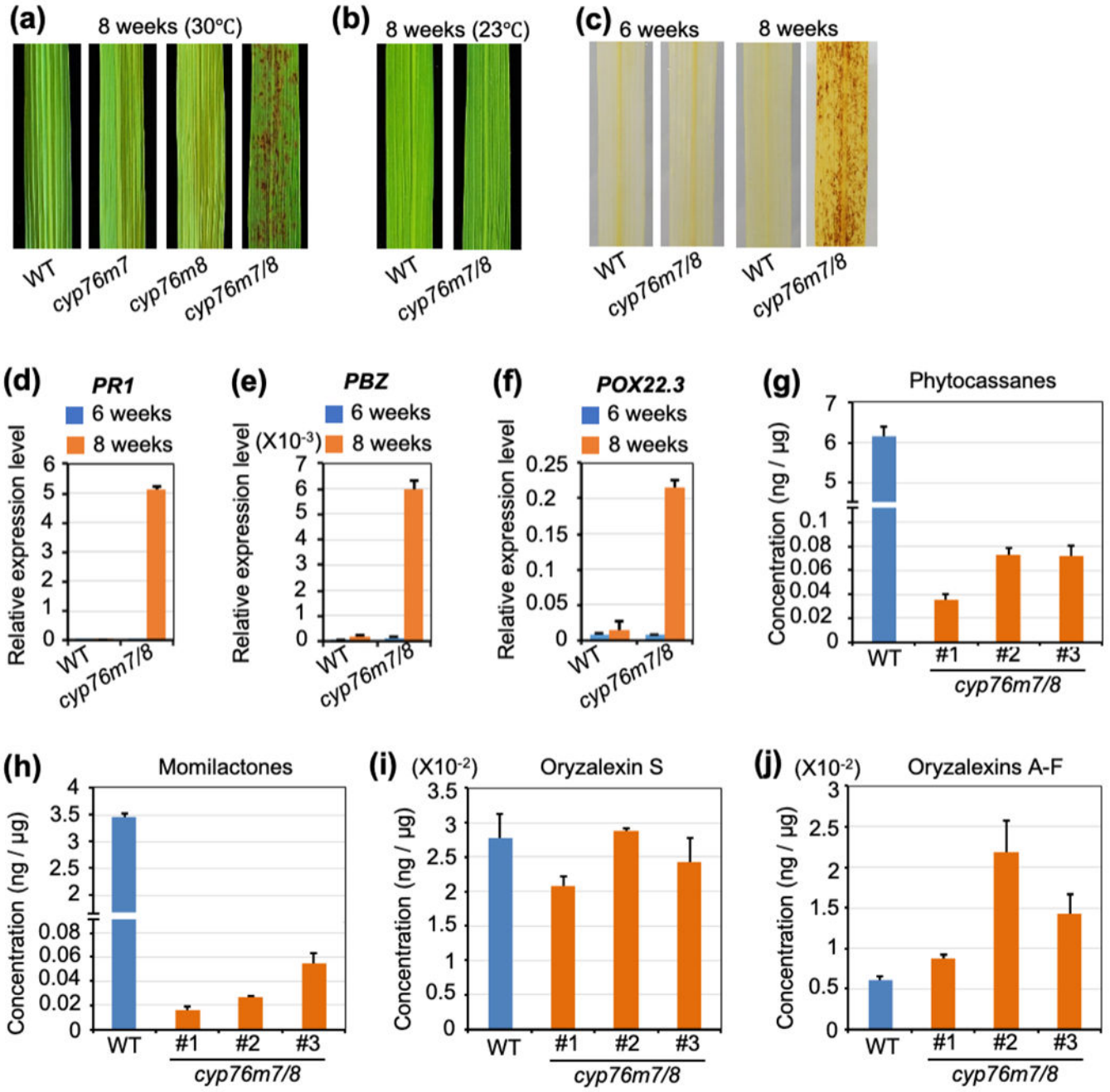


**Figure 6. Lesion mimic phenotypes and phytochemical profiling of rice double knockout mutants of *cyp76m7* and *cyp76m8*.**

(**a**) Representative leaves of wild-type (WT), *cyp76m7, cyp76m8* and *cyp76m7/8* plants grown in greenhouse (30 °C) two months after germination.

(**b**) Representative leaves from heading stage of WT and *cyp76m7/8* plants grown growth chamber at 23°C.

(**c**) DAB staining of *cyp76m7/8* and WT leaves before and after appearance of lesions.

(**d,e,f**) Relative expression level of defense-related genes, *PBZ*, *PR1* and *POX22-3* in leaves from *cyp76m7/8* plants compared to WT. The leaf tissues were sampled before (6 wks) and after (8 wks) formation of lesions, respectively. Error bars represent +/− SD.
(**g,h,i,j**) Effect of *cyp76m7/8* double knock-out on labdane-related diterpenoid metabolism relative to WT plants. Error bars represent +/− SD.

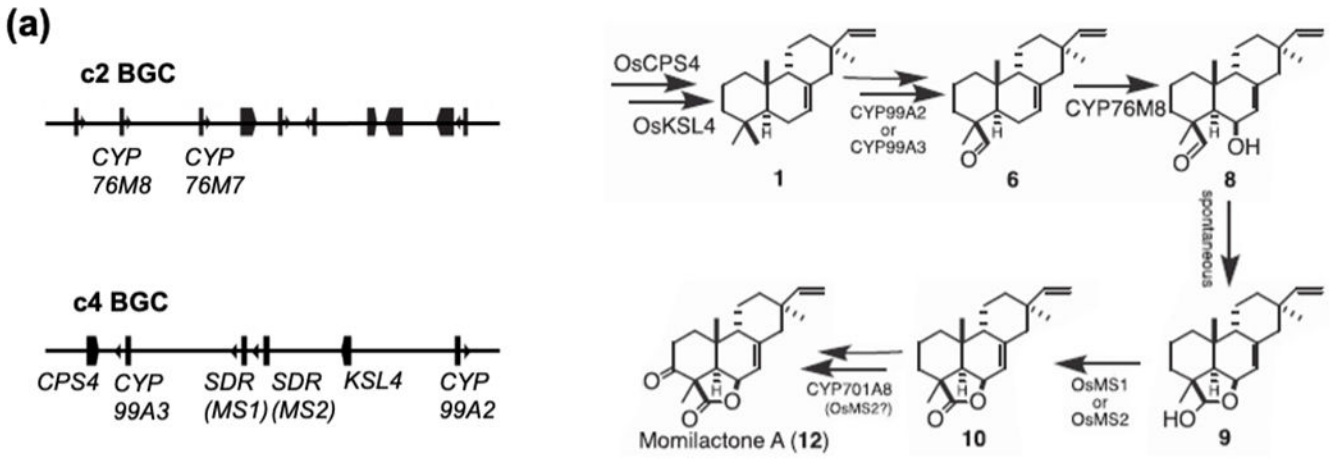


**(b)**

| Mutant | Phenotype (lesion mimic) | Conclusion |
|---|---|---|
| *cyp76m7* | No | *CYP76M7* and *CYP76M8* are redundant to each other. Lesion mimic should be due to intermediates or side-products in plants lacking CYP76M7 and CYP76M8 enzymes. |
| *cyp76m8* | No | |
| *cyp76m7/8* | Yes | |
| Δ*c2bgc* | Yes | Products from c2BGC are not essential for lesion mimic. |
| Δ*c4bgc* | No | Intermediates or side-products from c4BGC are essential for lesion mimic. |
| Δ*c2/c4bgc* | No | |
| *cps4* | No | |
| *cps2/cps4* | No | |

**Figure 7. Intermediates or side-products from c4BGC are genetically suggested to be reasons for lesion mimic in edited rice.**

(**a**) Genes from c2BGC (*CYP76M8*, plus *CYP76M7*) and C4BGC are collaborated in biosynthesis of momilactones.

(**b**) Lesion mimic phenotype of relative single, double mutants and BGC deletion mutants, which suggests intermediates or side-products from c4BGC are essential for lesion mimic.